Review

This project is focused on the study of a specific kind of DC to AC or AC to DC converter, named voltage ource converter (VSC), but specifically on the three-phase and two level version.

On the one hand, the fundamental structure and the operation principle will be explained more in depth. On the other hand, the Different applications of this converter will be seen with more emphasis through simulation.

For that purpose, this work is comprised by the following steps:

1. Study of the VSC structure and operating principle, which will be the main component of our systems, and study of the medium frequency transformer.

2. Study and simulation of the different control strategies.

3. Conclusions from the different simulated systems and control strategies, and review of the different features of the VSC and the transformer seen during the project.

The diferent models and simulations are done using Matlab, Simulink and Simpowersystems [1].

Summary

Preface

Origin of the project

This project is born from the constant technological improvement of electricity distribution technologies. Nowadays, new applications, like the smart grids, have appeared that require to have power converters and power transformers in order to be able to connect different kinds of energy sources to a common grid. That is the case of the renewable electricity generators like solar which is already direct, or the variable-speed wind turbine generators, which has to inevitably be rectified to dc for a modification process, and which then has to go back to AC, to connect to the grid

Motivation

Since the use of AC/DC type converters is very spread, there exist many different kinds of them. For that reason, it is interesting to make a more in depth study of these in order to know the different features they have. In this particular project, the chosen converter will be the VSC.

As far as personal motivations, there are mainly two. One is doing something related with renewable energies such as the wind power, since it is one of the fields I am more passionate about, and the other one is doing something in the field of electronics, which is one I have enjoyed studying through my years in the UPC.

Previous requirements

To work on this project, it is important to have a grasp on at least these two things:

1. Power electronics. Specifically on electrical energy converters and also on the

theory of transformers.

2. English. Since this project is both written and orally presented in English.

Chapter 1: Introduction

In this project, the two-level three-phase voltage source converter (VSC) is being studied in depth. Its structure, operating principle, and its self-commutated switches will be reviewed.

The modelling of the converter in connection to an AC grid will be built, and from there, different control strategies used for applications such as storage systems, and distributed renewable energy generation systems will be studied and subsequently implemented.

Finally, the addition of a transformer to the system will be simulated to see how its parameters affect the current and voltage on each of its sides and to see how that would translate to a three-phase Double Active Bridge (DAB3) converter, a DC/DC converter that has been tested to provide energy from a distributed wind power generator to a direct current grid [4].

Chapter 2: The VSC.

2.1 VSC model

2.1.1 Structure of the two-level three-phase Voltage Source Converter.

This specific case of Voltage Source Converter, is the simplest from all the three-phase VSC's.

Its structure is composed of three parallel branches, one for each phase, each of which contains two IGBT switches which are never be on or off at the same time.

Each of the IGBTs then has an anti-parallel diode connected to it, which conducts current when its IGBT doesn't.

On figure 1 we can clearly see all of the parts of the aforementioned structure of the VSC.

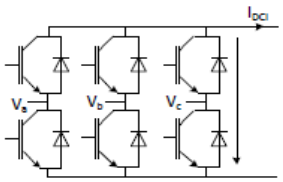

Fig 1: VSC internal model

2.1.2 Operating principle

Each of the three phases of the VSC corresponds to one of the three parallel branches, so once one of them has been studied and understood, the rest will be also. The only difference between each phase, will be that in order to create a three-phase balanced output, a lag between the commutations in each of the branches will have to exist.

To understand the concept, it is very helpful to see figures 2a and 2b:

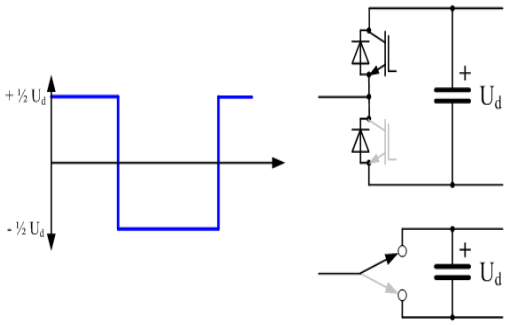

Fig. 2a: Upper commutation level[14]

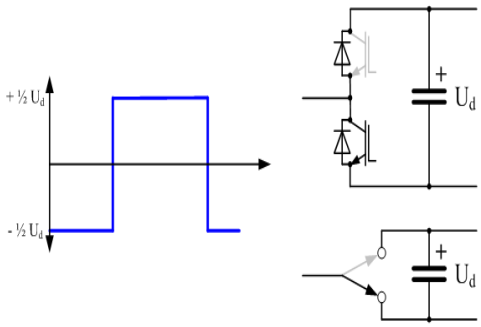

Fig. 2b: Lower commutation level [14]

Here, one of the branches is visualized, and the two commutation positions. The continuous switching creates an ondulating output signal that in thus making the DC/AC conversion happen.

2.1.3 The IGBT.

The Insulated Gate Bipolar Transistor or IGBT, is an electronic switcho in power electronic systems. The IGBT is composed by the combination of two other transistors. The N channel Metal-Oxide-Semiconductor Field-Effect Transistor or MOSFET and a PNP bipolar junction transistor or BJT, forming the structure seen in figure 5

.

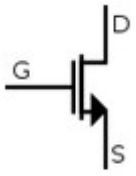

Fig. 3: N channel MOSFET

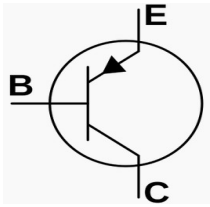

Fig. 4: PNP BJT

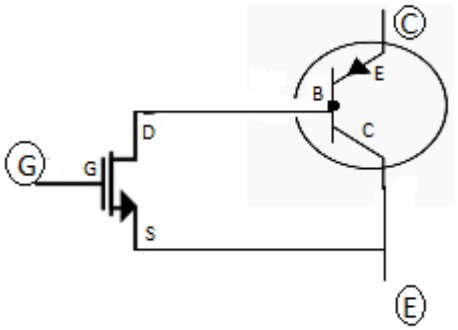

Fig.5: IGBT

The two interesting things of IGBTs are that they have the same gate as the MOSFET, providing a voltage control, and at the same time they have low losses like a BJT thanks to a small and constant tension Vce between the collector and emitter (C and E).

Figure 6 shows the different working regimes of a BJT, and the encircled zone, known as saturation, is the working zone wanted, for a BJT to act as a turned on switch. It is clear how the Vce voltage stays relatively small in that area, and specially so, if compared to a MOSFET's.

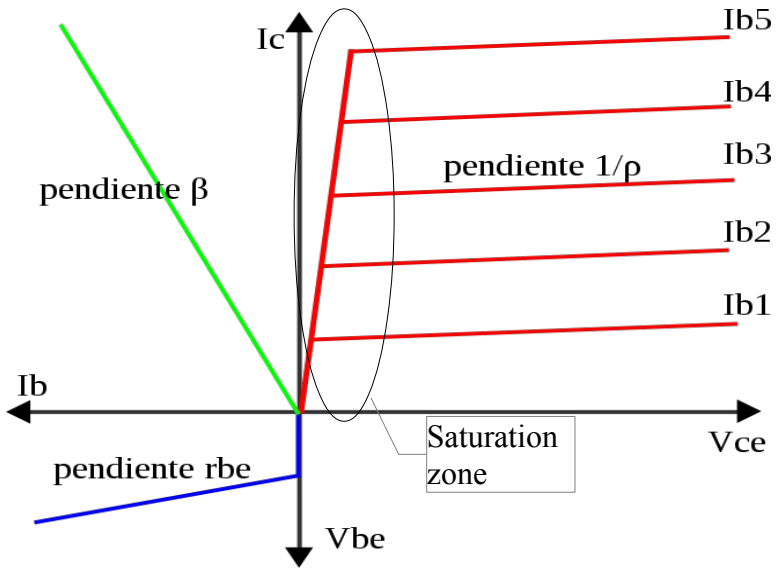

Fig. 6: [15]

2.2 Advantages and disadvantages of the VSC.

Usually, the alternative option to VSCs are Line Commutated Converters or LCCs.

LCCs use diodes, but mostly thyristors as their switching devices. Diodes are uncontrollable and thyristors can only be turned on, but not off, by control action.

Keeping that in mind, and knowing that the VSC uses IGBTs, the advantages it has are:

They are fully controllable due to the self-commutated switches.

The switches can be turned on and off at will, allowing to have the desired switching frequencies providing better harmonic performance, thus diminishing the need of filtering, which also allows for smaller size converters.

Unlike LCC's, VSC's don't depend on the grid they are feeding for the switching process to work, they can feed power to all kind of AC networks, included the ones compound only by passive loads.

The disadvantages of VSC in comparison to LCC, also exist and are:

Since VSCs use Pulse Width Modulation or PWM [7] in order to improve the harmonic distortion of the waves, the converters have to be switched many times on and off, leading to high switching losses in the IGBTs and loss of transmission efficiency. These losses are higher than those of LCCs

The voltage difference IGBTs can handle is lower to that of thyristors, so in high voltage applications many switches need to be connected in series and switched simultaneously increasing the level of complexity of the system and its electromagetic intereference levels.

2.3 Applications of a VSC

As already mentioned, the smart grid concept [8], is one that often uses AC/DC converters as seen on figure 7. Taking advantage of that, this project is going to focus particularly on two of these (the ones framed in red). One of them is the storage system, which is clearly seen from Figure 7 to be very similar to a photovoltaic generator, since they are both DC sources. And the other application will be the wind power energy generation system.

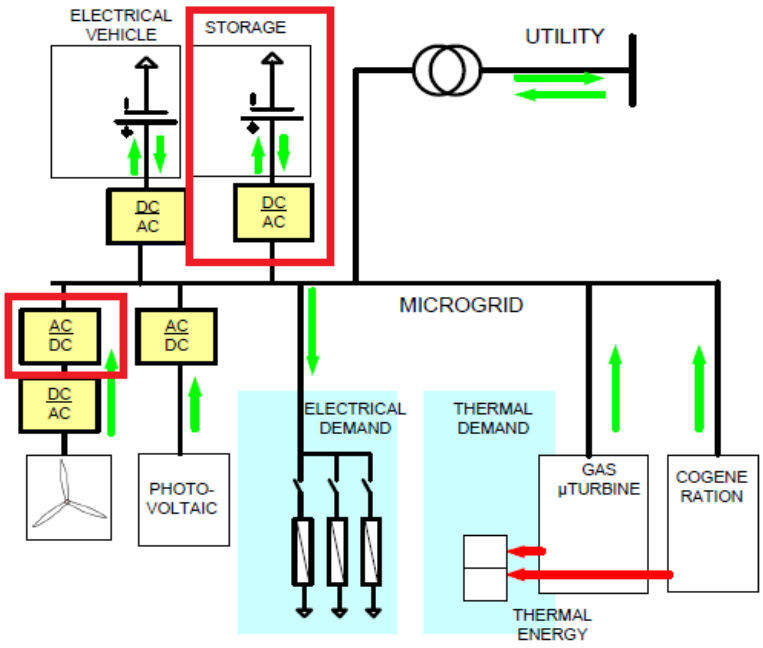

Fig. 7: Example of a grid with a storage and a generation system [6]

2.3.1 Storage systems.

The storage system objective is to be able to either draw, or inject power to the AC-grid through the active power reference value sign (P*). The VSC is able to provide that as it is bidirectional.

The control schemes required are the ones shown in figure 8. Although they will not be further analyzed until the next chapter, it must be said that the only actual controller is the current loop which controls the AC current to ensure power balance. The rest are set point calculations to enable or simplify the control operation.

Since the control is adjusted to charge the battery or to inject energy to the grid, the reference variables for the control will be the active power, in order to accomplish that, and the reactive power in order exchange with the grid upon requirement. Because the active power is a reference variable, and so it is already provided, the reference computation block will not need a DC voltage controller, thus simplifying its modeling.

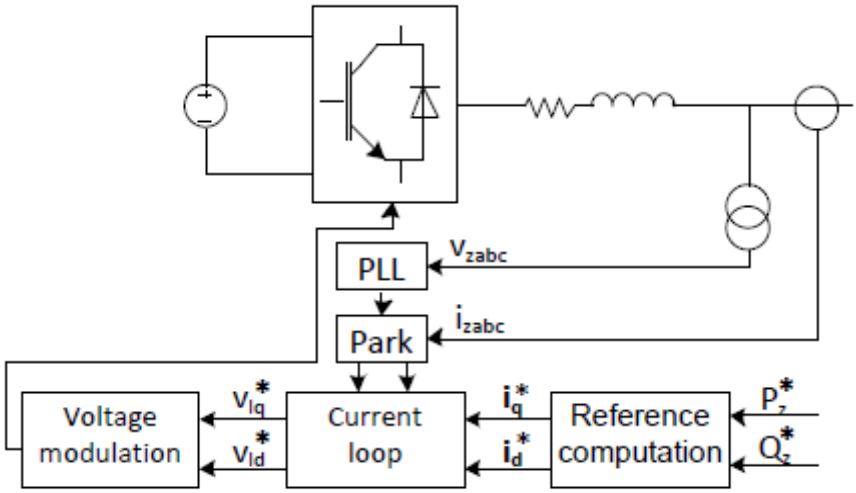

Fig. 8: Control scheme for generation storage systems. [6]

2.3.2 Distributed renewable energy generation system

Distributed energy is generated by a variety of grid-connected devices. In this case, the distributed energy resources are the different wind turbines of a wind power plant.

For this application the main interests are two.

Active power injection, which is performed by controlling the DC bus voltage.

In this case, the DC link which will be the wind turbine generator will be consisting of a controlled current source with a changing current reference value (Idc*) simulating the aforementioned fluctuating power flow, and a parallel capacitance smoothing the DC bus voltage as seen on figure 9. That way, the DC voltage value is not fixed, and the regulation of the DC bus voltage will be the DC bus voltage controller responsibility.

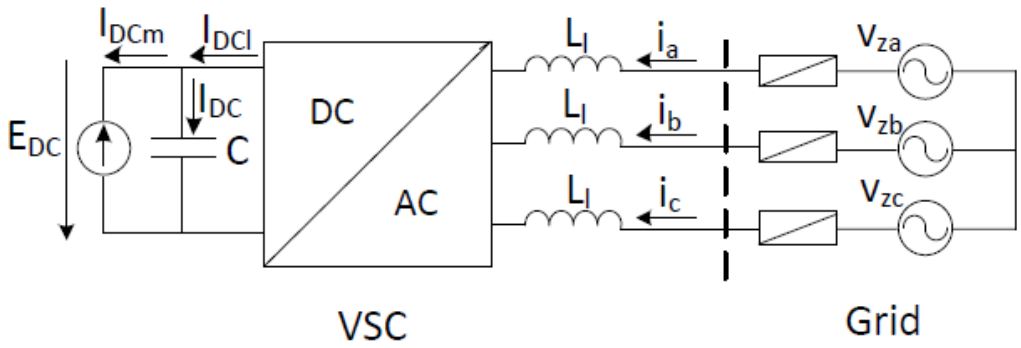

Fig. 9: DC generation, VSC, series inductances with losses (resistence blocks) and AC grid [6]

The second interest of the control is to ensure the power balance between grid and generation, as in the case of the storage system.

2.4 The three-phase dual active bridge (DAB3)

2.4.1 Electrical energy transmission with direct current (DC)

Even though direct current technology has been used for high voltage transmission purposes with line commutated converters (LCC) since the 1950's, and with voltage-source converters since the 1990's, it is not used to operate medium voltage collection grids in wind farms yet. The transition from HVDC to MVDC has its complexity, since HVDC vastly consists of point-to-point connections, and the concept of meshed grids is just now starting to be implemented.

DC technology has several advantages over AC technology. Tests have been made [2] demonstrating the increased power capability of a medium voltage single conductor cable when used with dc compared to ac (about a 1.56 ratio),

Some of the advantages of dc technology are the following:

- Reactive power is avoided since direct current does not produce it nor consume it (only active).

- Lower power losses in many different applications because direct current can be transmitted more effectively through cables (No skin-effect).

- The utilization of cable is improved [3].

2.4.2 Medium voltage DC application and the DAB3

There are many converters that have more than one conversion process in order to obtain the desired output. Apart from an AC/DC converter, the VSC can also be employed within other converters such as DC/DC converters that may need intermediate transformations to AC in order to, for example, step up the voltage through an AC transformer.

One case that has recently been studied, and can also have an application in the world of renewable energy like wind farms [9] and solar power plants [10] are the medium-voltage direct current (MVDC) collection grids, to transfer energy in DC instead of AC.

In order to implement an MVDC collector grid, it is key to have DC/DC converters with enough power capability and that can also step up the voltage levels of the source to make it compatible with the DC distribution grid. One of the cases studied to serve that purpose is the three-phase dual active bridge (DAB3) converter seen on figure 10.

The DAB3 contains two VSCs, one to make the DC/AC conversion, and another to rectify the AC to allow the connection to the DC grid. The DAB3 also contains a transformer to provide the voltage increase and the galvanic isolation.

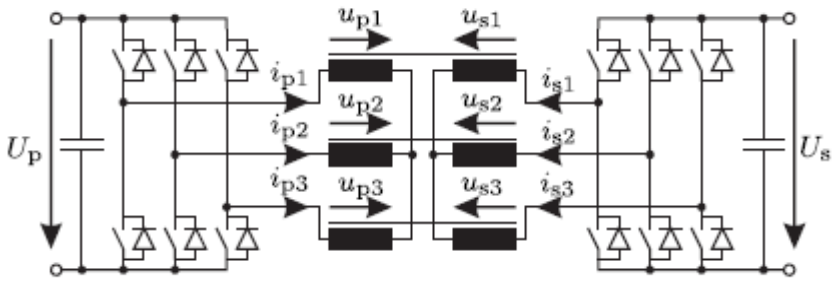

Fig. 10: DAB3 internal model [5]

In order to expand the scope of the project, further investigation will be carried out to understand the transformer's operation principle, its integration to the system, and the effects of parameter changes on the results obtained.

Chapter 3: Simulation of the different controls.

3.1 Transformation of instantaneous electrical quantities.

For the controller designs, dealing with constant values is helpful, but many of the currents and voltages on the following simulations are sinusoidal signals.

To obtain constant values the instantaneous power theory [11] and the αβ0 and dq0 transformations Are used and presented in the following.

3.1.1 Instantaneous power theory on the αβ0 frame.

The clarke transformation (αβ0) transforms quantities in the abc three-phase reference frame to an αβ0 ortogonal reference frame.

$$\begin{bmatrix} x_\alpha \\ x_\beta \\ x_0 \end{bmatrix} = \frac{2}{3} \begin{bmatrix} 1 & -\frac{1}{2} & -\frac{1}{2} \\ 0 & \frac{-\sqrt{3}}{2} & \frac{\sqrt{3}}{2} \\ \frac{1}{2} & \frac{1}{2} & \frac{1}{2} \end{bmatrix} \begin{bmatrix} x_a \\ x_b \\ x_c \end{bmatrix}$$

$$\begin{bmatrix} x_a \\ x_b \\ x_c \end{bmatrix} = \begin{bmatrix} 1 & 0 & 1 \\ -\frac{1}{2} & -\frac{\sqrt{3}}{2} & 1 \\ -\frac{1}{2} & \frac{\sqrt{3}}{2} & 1 \end{bmatrix} \begin{bmatrix} x_\alpha \\ x_\beta \\ x_0 \end{bmatrix}$$

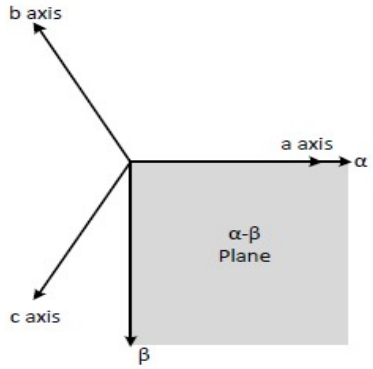

Fig. 11 αβ0 plane

Using the instantaneous equations and applying them for the systems AC voltages and currents, the following αβ0 equations are obtained:

$$x_a(t) = \sqrt{2}X\cos(\omega t + \phi)$$
$$x_b(t) = \sqrt{2}X\cos\left(\omega t + \phi - \frac{2\pi}{3}\right)$$
$$x_c(t) = \sqrt{2}X\cos\left(\omega t + \phi + \frac{2\pi}{3}\right)$$

Eq. 1

$$x_\alpha = \sqrt{2}X\cos(\omega t + \phi)$$
$$x_\beta = -\sqrt{2}X\sin(\omega t + \phi)$$
$$x_0 = 0$$

Eq. 2

Where xo = 0 because both the voltages and the currents are balanced.

Then, defining the voltage and current phasors as:

$$\sqrt{2}\underline{I}^{\alpha\beta} = i_\alpha - ji_\beta$$

Eq. 3

$$\sqrt{2}\underline{V}^{\alpha\beta} = v_\alpha - jv_\beta$$

Eq. 4

The complex power expression will be:

$$\underline{S} = P + jQ = 3\underline{V}^{\alpha\beta}\underline{I}^{\alpha\beta *} = 3\left(\frac{v_\alpha - jv_\beta}{\sqrt{2}}\right)\left(\frac{i_\alpha + ji_\beta}{\sqrt{2}}\right)$$

Eq. 5

That can be decoupled as:

$$P = \frac{3}{2}(v_\alpha i_\alpha + v_\beta i_\beta)$$
$$Q = \frac{3}{2}(v_\alpha i_\beta - v_\beta i_\alpha)$$

Eq. 6

These quantities in the αβ0 frame are still variable in steady state. The alpha beta 0 quantities reduce the number of variables from three to two. For control purposes, constant quantities are necessary which can be obtained by the Park transformation.

3.1.2 Transfer to the qd0 frame (Park transformation)

The park transformation can also be described in geometrical terms as the clarke transformation plus a rotation (Figure 12). By choosing the right rotation angle, the values in the qd0 frame will turn out to be two constant value, Vq and Vd, and not only that, but Vd will also be controlled to zero (figure 13) by an appropriate phase tracking unit (phased-locked loop, PLL),

All of that applies during steady state conditions, but since the distribution grid is always on steady conditions, unless a fault occurs, the tensions will remain constant.

$$T(\theta) = \frac{2}{3}\begin{bmatrix} cos(\theta) & cos\left(\theta - \frac{2\pi}{3}\right) & cos\left(\theta + \frac{2\pi}{3}\right) \\ sin(\theta) & sin\left(\theta - \frac{2\pi}{3}\right) & sin\left(\theta + \frac{2\pi}{3}\right) \\ \frac{1}{2} & \frac{1}{2} & \frac{1}{2} \end{bmatrix} \qquad [x_{qd0}] = [T_{qd0}]\,[x_{abc}]$$

$$T^{-1}(\theta)\begin{bmatrix} cos(\theta) & sin(\theta) & 1 \\ cos\left(\theta - \frac{2\pi}{3}\right) & sin\left(\theta - \frac{2\pi}{3}\right) & 1 \\ 1 & & \\ cos\left(\theta + \frac{2\pi}{3}\right) & sin\left(\theta + \frac{2\pi}{3}\right) & 1 \end{bmatrix} \qquad [x_{abc}] = [T_{qd0}]^{-1}\,[x_{qd0}]$$

Eq. 7 *Eq. 8*

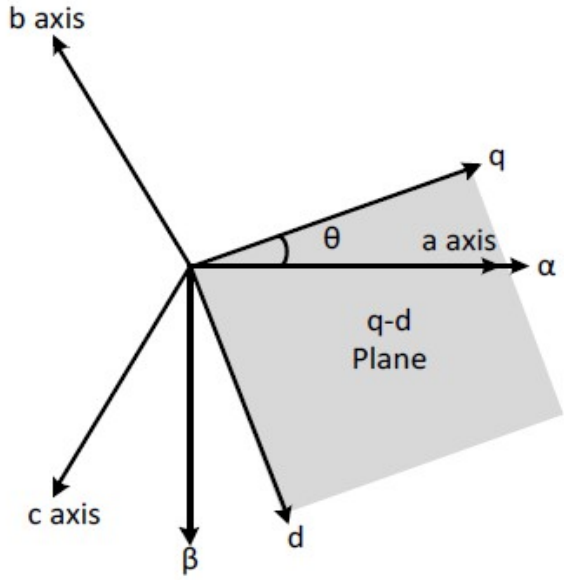

Fig. 12 qd0 and αβ0 frames.

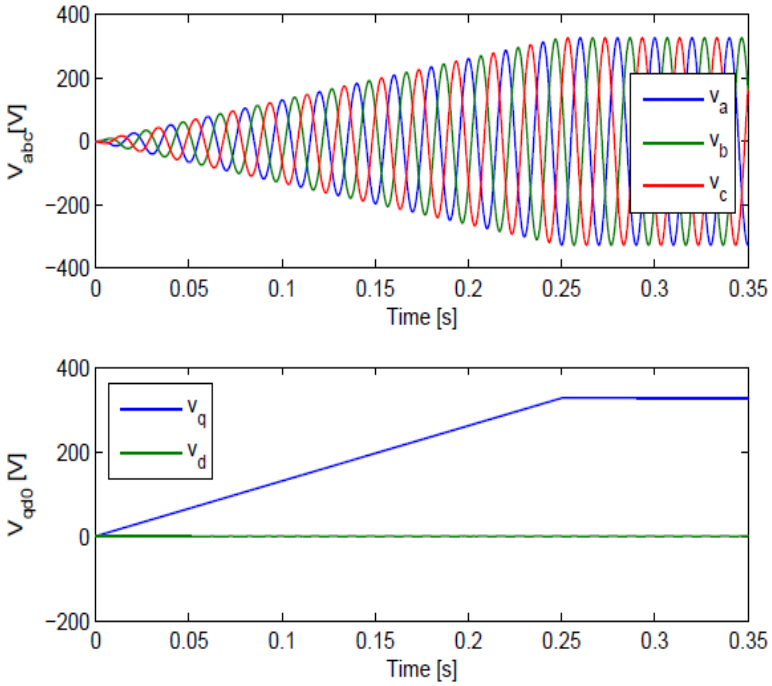

Fig. 13: Voltages in the abc and qd0 frames [6]

Finally, as in the clarke transformation the following equations are obtained:

The current and tension phasors:

$$\underline{V}^{qd} = \frac{v_q - jv_d}{\sqrt{2}}$$

$$\underline{I}^{qd} = \frac{i_q - ji_d}{\sqrt{2}}$$

Eq. 9:

The complex power:

$$\underline{S} = P + jQ = 3\underline{V}^{qd}\underline{I}^{qd*} = 3\left(\frac{v_q - jv_d}{\sqrt{2}}\right)\left(\frac{i_q + ji_d}{\sqrt{2}}\right)$$

Eq. 10

And the decoupled active and reactive power:

$$P = \frac{3}{2}\left(v_q i_q + v_d i_d\right)$$

$$Q = \frac{3}{2}\left(v_q i_d - v_d i_q\right)$$

Eq. 11

3.2 Operation model (grid, converter and DC link)

3.2.1 AC grid modeling.

For grid modeling purposes, the circuit on figure 14 will be implemented in simulink in order to display the different grid configurations and its voltages and currents.

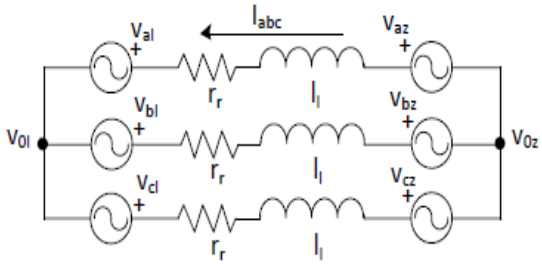

Fig. 14: AC side of the VSC and grid [6]

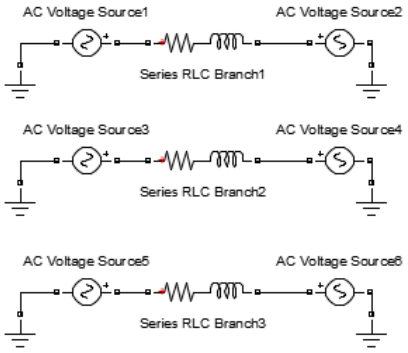

Fig. 15: simulink model of Figure 14

The modelled voltage sources are all of a fixed kind. Three of them act like the AC grid, and the other three as the VSC's AC side.

The windings between the sources are used to decouple them, and they also allow to control the transferred power.

$$P = \frac{U^2}{X} \cdot \sin(\theta)$$

Eq. 12

$$X = w \times L$$

Eq. 13

$$U = L \times \left(\frac{di}{dt}\right)$$

Eq. 14

The resistences are there simply to simulate some transmission losses.

Something to take note of, is that since the Park transformation for power electronics in Simulink is rephrased as dq0 instead of qd0, and even the Park transformation block supports this notation, further experimentation with Matlab Simulink and

Simpowersystems will be carried out using the dq0 frame aswell.

The first thing to notice is that a voltage difference between the set of voltage sources will cause a current through the impedance. If the voltages of both of each phase's sources are of the same peak value and phase angle, the resulting current will be zero.

Another thing taken away, is that in order for the Vd, Vq to be constant values, and V0 to be equal to zero, the grid voltages must be balanced (the three signals phases must be separated by 120 degrees to each other). An example is Figure 16 where the AC grid has the following values:

	Source 1	**Source 3**	**Source 5**
Peak Amplitude (V)	100	100	100
Phase (deg)	30	-90	150
Frequency (Hz)	50	50	50

Table 1: AC grid values

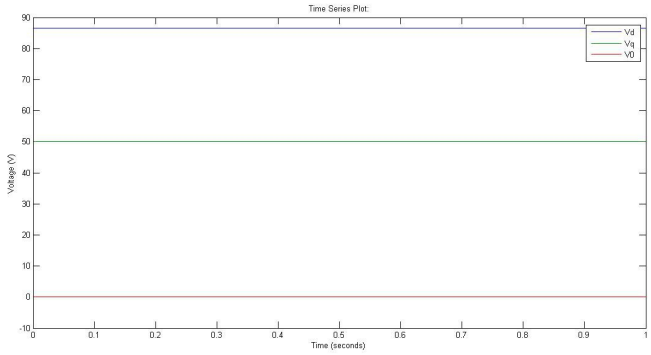

Fig. 16: dq0 tensions with values from table 1

Finally, if the three phases add to zero ($\sum\varphi i=\varphi 1+\varphi 2+\varphi 3=0º$), then Vq can be controlled to zero, as seen on Figure 17 where $\varphi 1= 0º$, $\varphi 2=-120º$, $\varphi 3=120º$.

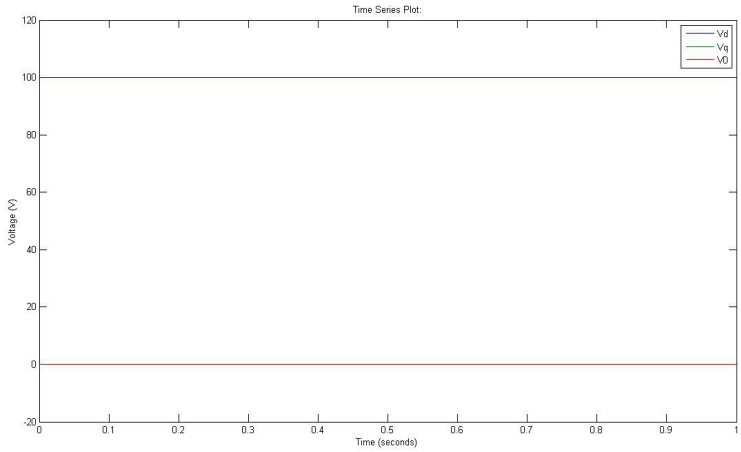

Fig. 17: dq0 tension values with new phases

With this test, since the AC grid will continue being modelled by voltage sources of fixed values, and for the sake of simplicity, in this work it is assumed to know the phase angle and frequency of the AC grid voltages which allow to neglect the use of a phase locked loop (PLL).

3.2.2 Converter modeling.

The modelling of the different switches of the VSC is not among this project goals.

If the real aim of this project is taken into account, there are two valid and simple ways to model the converter that are going to be used.

The first one is only possible in the storage system model, since the other model needs the current source to be able to apply the reference current (Idc*). The idea is to simply model the AC side of the VSC as controlled AC voltage sources, and to have no DC link. That way the control has to provide the desired AC side voltages to these controlled sources in order to ensure the wanted resulting P and Q.

The other option is to use the Universal bridge block found in the Powerlib Simulink library. That block can simulate an Average-model based VSC which acts like the previous option, but with the difference that it is coupled to a DC side, and the power balance between the two sides is always fulfilled. That simplifies the job, since the simulation of the switches and gating signals is not relevant to this work as already

explained.

3.2.3 DC link modeling.

In the models including the VSC block, a DC link will also be needed.

As mentioned in the previous chapter, the storage system control will require a DC voltage source. Thus the DC link's simulation will be exactly that.

In the distributed renewable energy generation system, the DC link has to be a current source because, as also mentioned in the previous chapter, the aim of the control is to regulate the DC bus voltage, and having already a voltage source, that control wouldn't be necessary. The problem here lies in the fact that the DC circuit would be composed by the VSC, acting as a direct current source, and the DC link current source, and a system can not have two current sources in series to eachother. For that reason, a parallel capacitance will be added.

3.3 Storage system control.

3.3.1 Storage system model.

The storage system can be modeled in two different ways with very similar results. These were already mentioned in the point 3.2.

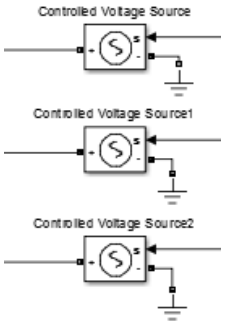

Fig. 18: VSC as controlled current sources

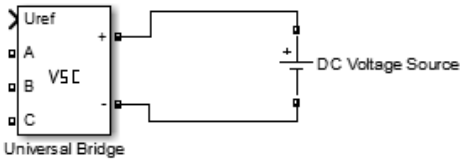

Fig. 19: VSC as a universal bridge and a dc voltage source

The AC grid used here and in all of the next simulations will have the following parameters:

- Peak tension: 350 V
- Phases: φ1= 0º, φ2=-120º, φ3=120º
- Frequency: 50 Hz

And the resistence and inductance values will be:

- R=0.5 Ω
- L=5.4 mH

3.3.2 Storage system control blocks.

The reference computation block will receive the two reference variables P* and Q* seen on Table 2, and the AC grid's voltages in dq0 frame and will provide the new id* and iq*.

Since Vq=0 V, the new power equations in the dq0 frame are simplified:

$$P=(\frac{3}{2})\times(Vq\times Iq+Vd\times Id)=(\frac{3}{2})\times(Vd\times Id)$$

Eq. 15

$$Q=\frac{3}{2}\times(Vq\times Id-Vd\times Iq)=\frac{3}{2}\times(Vd\times Iq)$$

Eq. 16

	P* [KW]	Q* [KVAr]
t=0 s	-3000	0
t=0.3 s	-6000	-5000
t=0.5 s	-1000	0
t=0.8 s	-7000	2000
t=0.9 s	-7000	-7000

Table 2: Active and reactive power references

Finally, there is the current loop block that provides the reference voltages values to inject to the VSC [6].

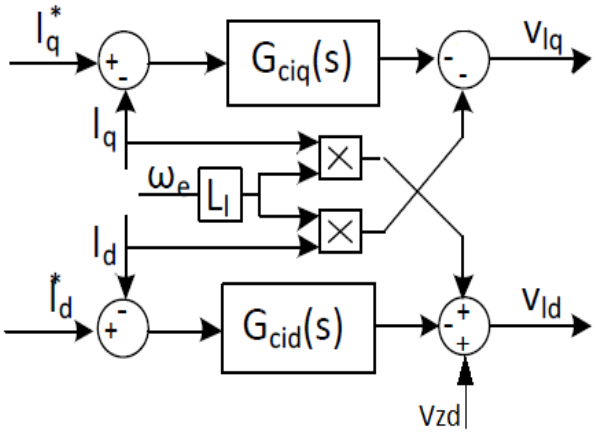

Fig. 20: Current loop

Gciq and Gcid are two PI controllers $G = Kp + \frac{Ki}{s}$ (In fourier)

Eq. 17

$$K_p = \frac{l_l}{\tau}$$
$$K_i = \frac{r_l}{\tau}$$

Eq. 18

And the current loop's time constant, which must be considerably faster (usually around 10x faster) than the converters swithing, is going to be τ=10 ms for this simulation.

The ωe seen on Figure 20 is the system's switching frequency ωe= 2*π*f=100*π.

The simulated control loop and the current loop eventually look like figure 21 and 22.

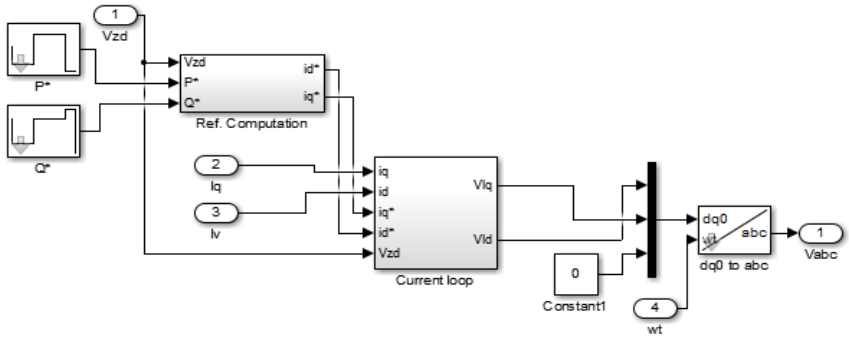

Fig 21: Control Loop

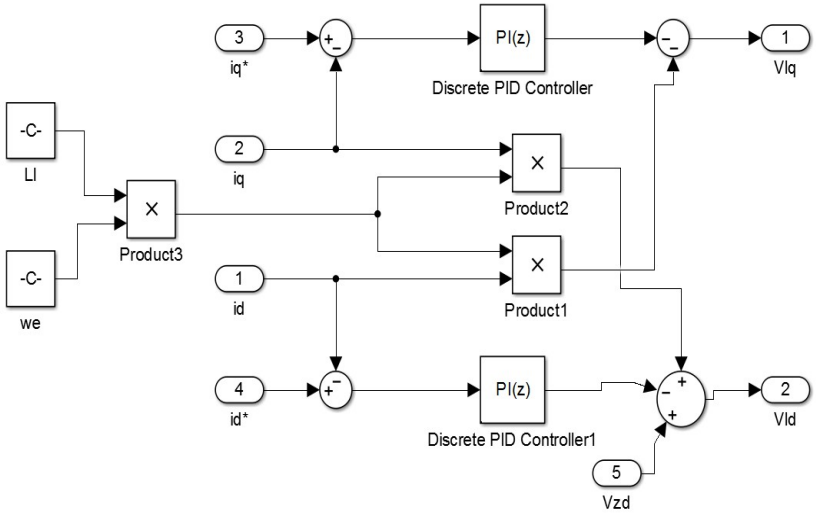

Fig. 22: Current loop

3.3.3 Storage system simulation results.

Since the two converter models use the same control, they can both be simulated by simply exchanging them on the exact same model. The results of the simulation are going to be shown in the following.

For the simulation, the settings of the model are going to be like the Powergui block in

figure 23.

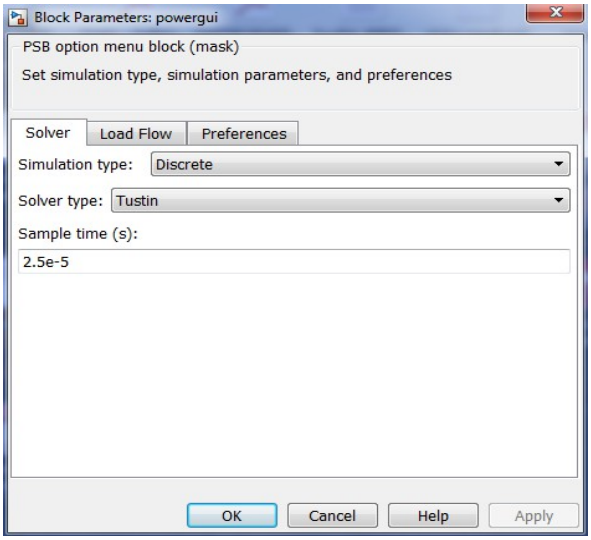

Fig. 23: Powergui setup

The solver configuration will look like figure 24.

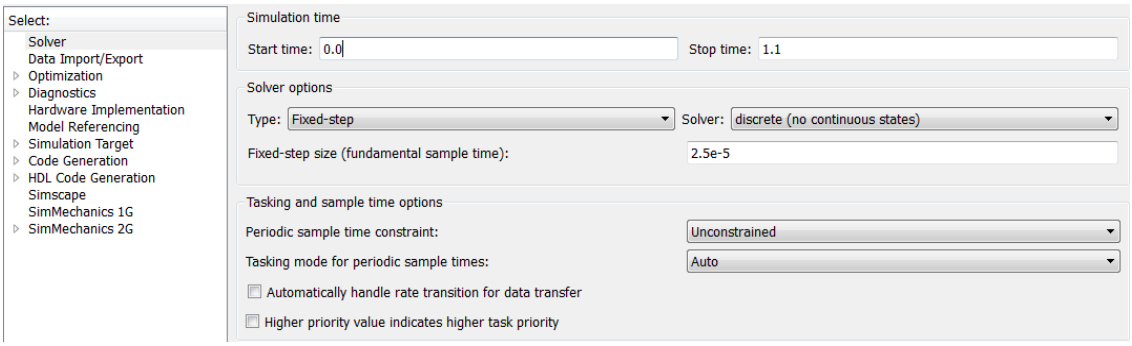

Fig. 24: Solver configuration

The solutions provided by the simulation can be seen here:

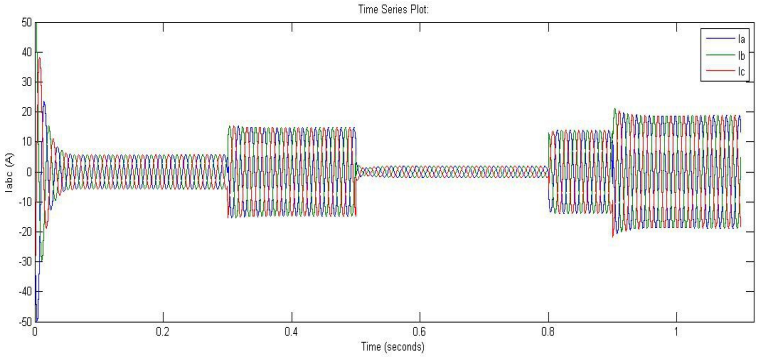

Fig. 25a: Iabc

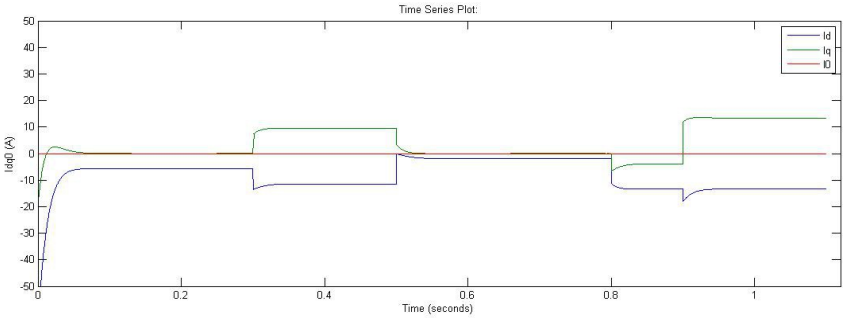

Fig. 25b: Idq0

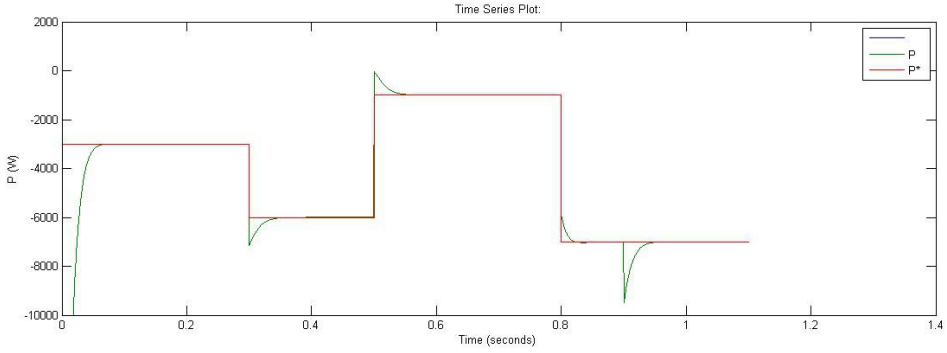

*Fig. 25c: P and P**

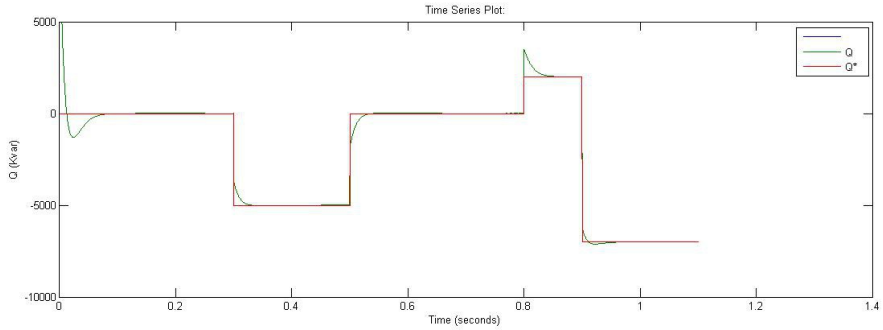

*Fig. 25d: Q and Q**

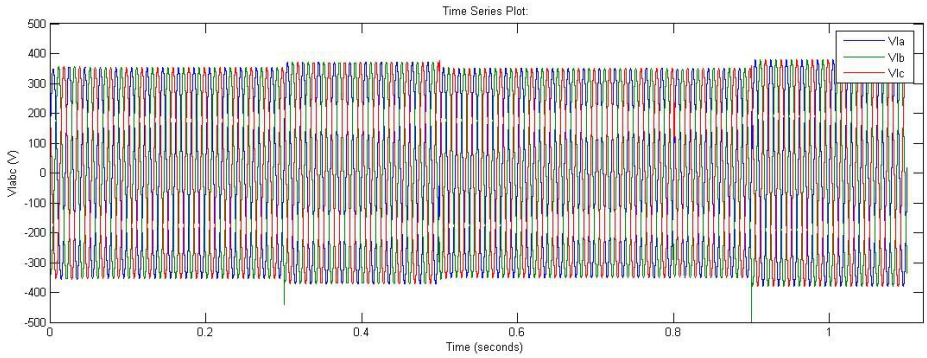

Fig. 25e: VSC AC link voltages (Vlabc)

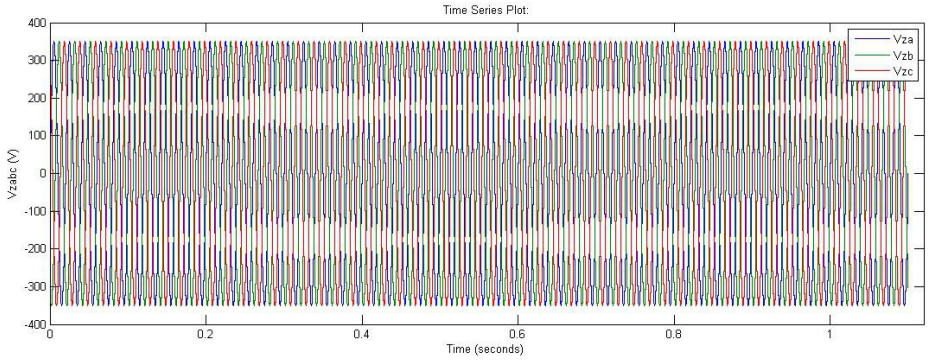

Fig. 25f: AC grid tensions (Vzabc)

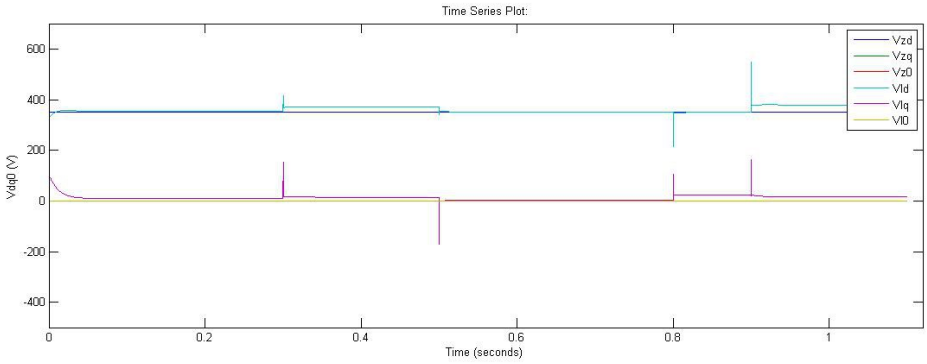

Fig. 25g: Vzdq0 and Vldq0

Figures 25a and 25b show the AC side currents in both abc and dq0 frames. The adaptation of the currents to the sudden reference changes can be appreciated, and they show great promise due to the speed at which the currents adapt and the almost none existing transient stage

It is also interesting to see how on figures 25c and 25d the P and Q measured in the simulation are very similar to the reference ones. In the event of a reference change, there appear some spikes which aren't desired. They are due to the AC link voltage spikes seen in figure 25e. Apart from that, the system adapts quickly thanks to the control.

Another interesting thing to take note off is that, with the exception of the reference change spikes, the peak AC tension on the AC link seen on figure 25e can not be higher than half of the DC bus voltage as figure 2 on section 2.1.2 shows.

$$V_{AC.peak} < \frac{V_{DC}}{2}$$

Eq. 19

Figure 25f shows the AC grid abc voltages, and they work as intended. Since they are fixed by the voltage sources, they are safe from any sort of eventuality.

Figure 25g also shows the spikes on the AC link's dq0 frame tensions when the reference values change, and the difference between the AC link and the grid due to the RL branches in between,

In general, the results are good. The signal tracking by the current loop is quite fast, and the measurements made during the simulations are well done, since the active and reactive power measured are emulating well the references, and the dq0 frame tensions are also matching well.

3.4 Distributed renewable energy generation system

3.4.1 Distributed generation system model.

As previously mentioned, this application will run a DC link composed by a current source and a parallel DC smoothing capacitor C=0.1 F.

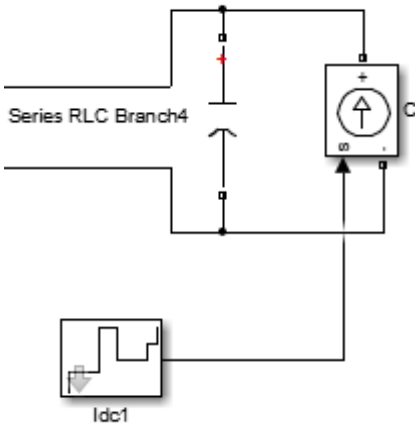

Fig. 26: Distributed renewable energy generation system converter DC link

Meanwhile the rest of the parts from the storage system model of section 3.3 will remain untouched.

3.4.2 Distributed generation system control blocks.

	Idc [A]	Q* [Kvar]
t=0s	0	0
t=0.1s	3	0
t=0.4s	10	0
t=0.6s	5	-5000
t=0.9s	7,5	-5000
t=1s	10	0

Table 3: Reference current and reactive power

The reference computation block will stay the same, but since the new reference variables are now Idc* and Q* seen on table 3, instead of P* and Q*, the reference P* will be obtained through a new control scheme called the DC voltage regulator [6].

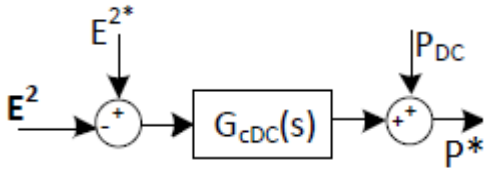

Fig. 27: DC voltage regulator scheme

Where E is the actual DC voltage of the DC link, and E* is the desired DC link voltage (Edc*=800 V).

GcDC will be a PI controller to control the input error to zero.

$$K_{pDC} = C\xi_E\omega_E$$
$$K_{iDC} = \frac{C\omega_E^2}{2}$$

Eq. 20 and 21

Where the voltage regulator parameters are:

- Damping coefficient: ξ_e=0.707
- Natural oscillation frequency: ω_n=1/0.15 rad/s.

Thus its frequency is $\omega_e = \omega_n \times \sqrt{1-\xi^2} = 4{,}71\, rad/s$

Eq. 22:

And K_{pdc}=0.332997; K_{idc}=1.109205 according to equations 20 and 21.

Since the outer voltage loop has to be much slower than the current control in order to assure stable system response (5-10x), the time constant has to be modified to fulfill that. Due to the frequency value (ω_e) of the DC bus regulator, the new time constant will be τ = 1 ms. That makes the Kp and Ki in the control loop ten times bigger than in the storage system: Kp = 5.4; Ki = 500

3.4.3 Distributed generation system simulation results.

The simulation configuration remains the same as explained in section 3.3.3

In the following graphics the different variables in the simulation can be better appreciated,

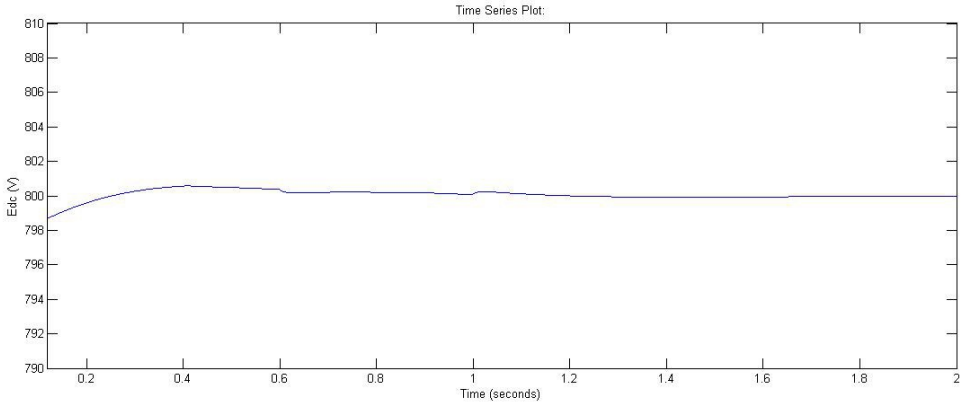

Fig. 28a: Edc

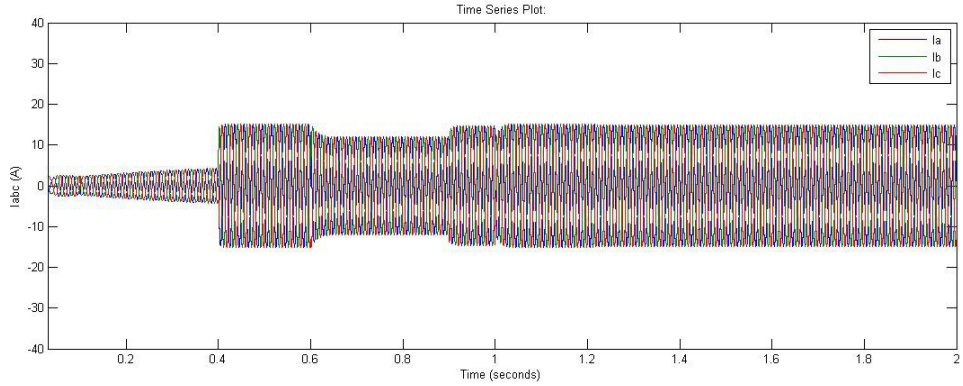

Fig. 28b: AC link abc currents (Iabc)

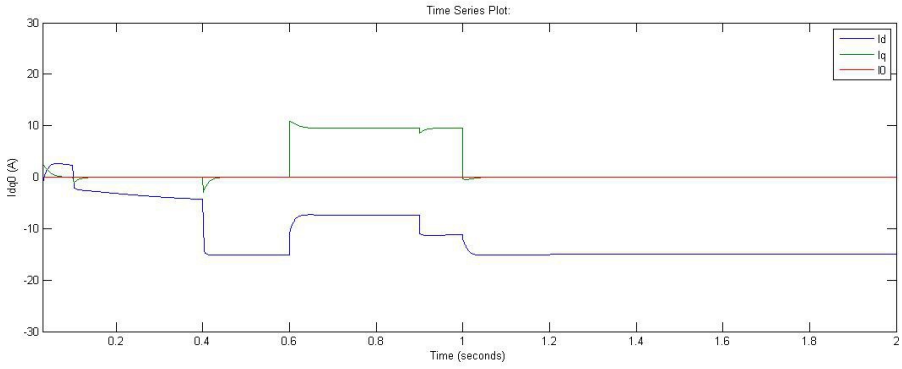

Fig. 28c: dq0 frame currents

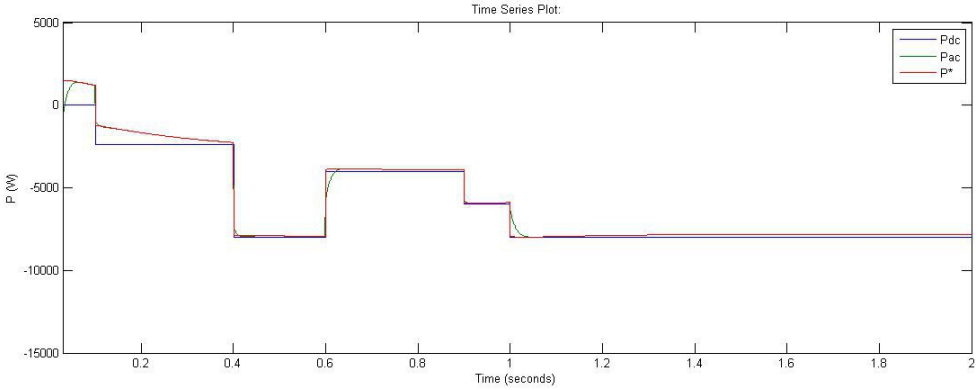

Fig. 28d: Active power (P) of converter DC link, AC grid and reference

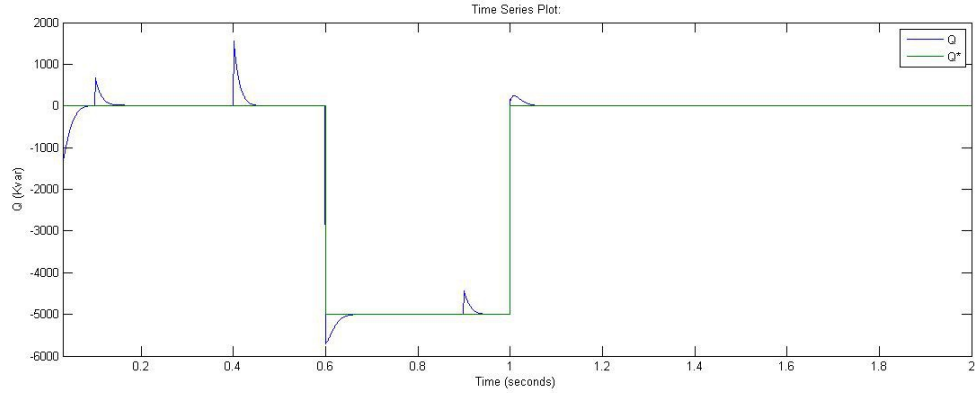

Fig. 28e: Reactive power (Q) of AC grid and reference

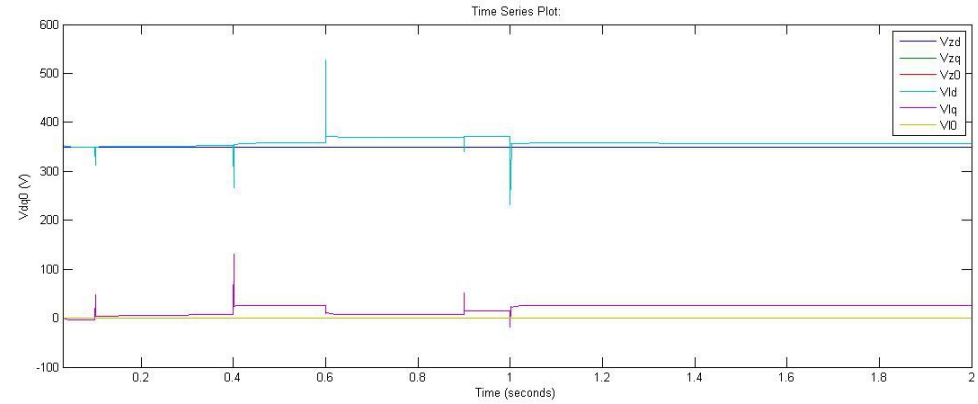

Fig. 28f: AC grid and converter AC link dq0 frame voltages

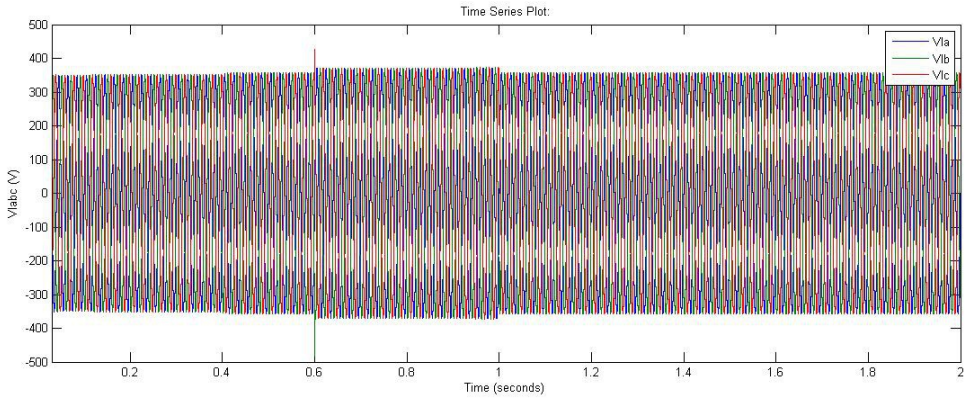

Fig. 28g: Converter AC link three-phase voltages (Vlabc)

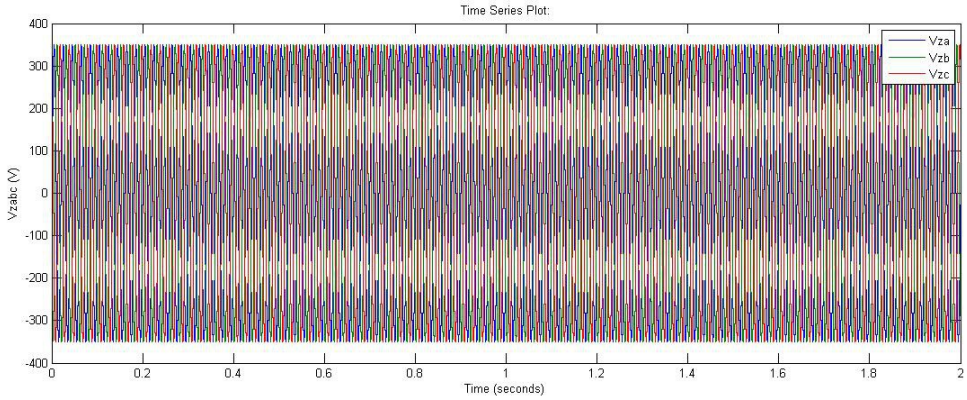

Fig. 28h: AC grid voltages (Vzabc)

In figure 28a the DC voltage is shown. The variation is smaller than 1% and the control achieves to stabilize the voltage to the reference of 800 V.

Figures 28b and 28c show the AC side currents in both abc and dq0 frames. The adaptation of the currents to the sudden reference changes is working fast and without much instability during the transient stages.

The Power balance is also achieved, as seen in figure 28d where the DC and AC sides show the same active power.

On figure 28e, the reactive power control is achieved since the measurements on the AC side tracks the provided reference well.

Figures 28d and 28e, show how both active and reactive power spike on the event of

reference changes due to the voltage spikes in the AC link of the VSC seen in figures 28f and g. Taking into account the rough and sudden nature of these reference changes, comparable to real life fault situations, these spikes are quite controlled, and the adaptation of the measured values to the new references is relatively fast.

Figure 28g also shows how equation 19 has to be fullfilled in this case as well as in the storage system.

On the other hand. the AC link voltages in both the dq0 and abc frames from figures 28f and 28g show significant spikes when the references change. Apart from that, the measurements taken are working well since the Vd and Vq tensions from the AC link match with the values from the AC grid. Also the effect on the voltage made by the series impedances is visible.

3.5 Model with transformer

3.5.1 Transformer structure

As explained in section 2.4, further investigation on the transformer will be carried out in order to understand how it will work on a three-phase Dual Active Bridge (DAB3).

In this case, the transformer will be set up between the VSC AC link and the AC grid on the distributed renewable energy generation system.

To do so, the three-phase transformer model from Simpowersystems will be used (Figure 29).

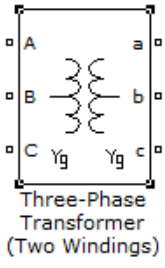

Fig. 29: Transformer Simulink block

With this block, the structure of the transformer can be specified. The transformer will be defined with the following parameters:

The first winding will be connected to the electrical grid. It isconnected in a triangle shape (D1). The secondary winding will be connected to the converter's AC link and will have a Yg structure (grounded star) providing a grounding. The D1 structure has its voltages lagging 30 degrees in comparison to the reference voltages in the Y winding, hence the name refering to the 30 degree phase lag of a clock needle at 1 hour compared to 12 hours. Being of the Delta – star kind, the structure of the transformer (D1yg) is one of the most common ones for power export applications, and thanks to having the y winding, the third harmonics are nullified [13].

Figure 30 shows the structures of the three-phase windings in D and Y connections.

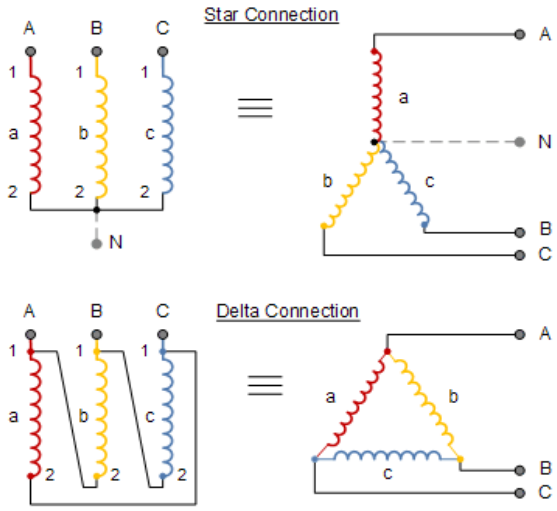

Fig. 30: Star and delta three-phase winding connections [12]

This simulation will be one step away from the actual DAB3. That step would be the addition of a second VSC in order to complete the DC/DC conversion, although in that case, a new control would be needed, and the transformer's windings would have a not grounded Y/Y structure Instead. in this case the stepped up voltages that are going to be studied will be the ones on the primary and secondary sides of the transformer. Using the formulation for Y/Y transformers instead of D1/Yg, these voltages are the DAB3's intermediate AC/AC conversion.

Figure 31 shows the conversions to calculate the transformer's line to line and line to phase voltages.

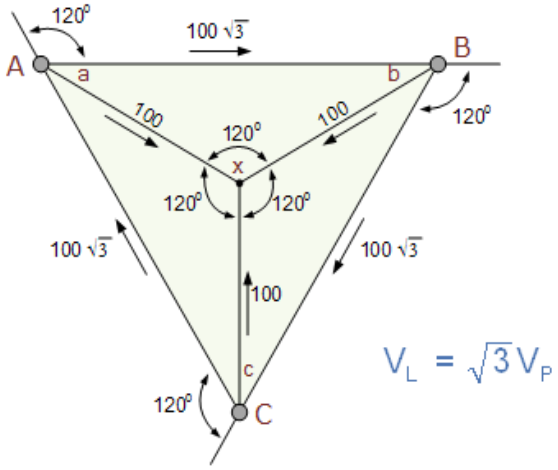

Fig. 31: Line to line and line to phase voltage conversions [12]

And table 4 shows that, and the line to line and line to phase transformer currents too.

3.5.2 Results of the simulation with transformer.

The primary side of the transformer has a line to neutral peak voltage of 350 V, therefore, and using equations 23 and 24:

$$V_L = V_{\ln} \times \sqrt{3}$$ *Eq. 23*

$$V_{rms} = \frac{V_{peak}}{\sqrt{2}}$$ *Eq. 24*

the phase to phase peak and rms voltage in the primary side will be: V_{p_peak}=606 V

V_{p_rms}=428,6 V.

For that reason the transformer values are the ones on figure 32

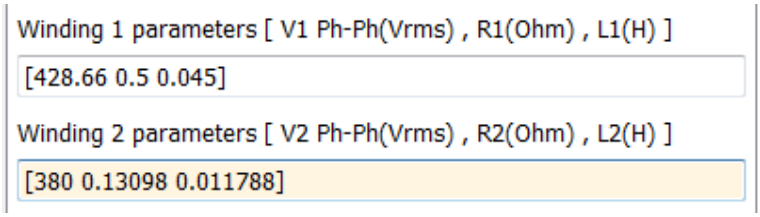

Fig. 32: Transformer parameters

A v1/v2 ratio of 428.66 V / 380 V, and small stray impedances have been chosen.

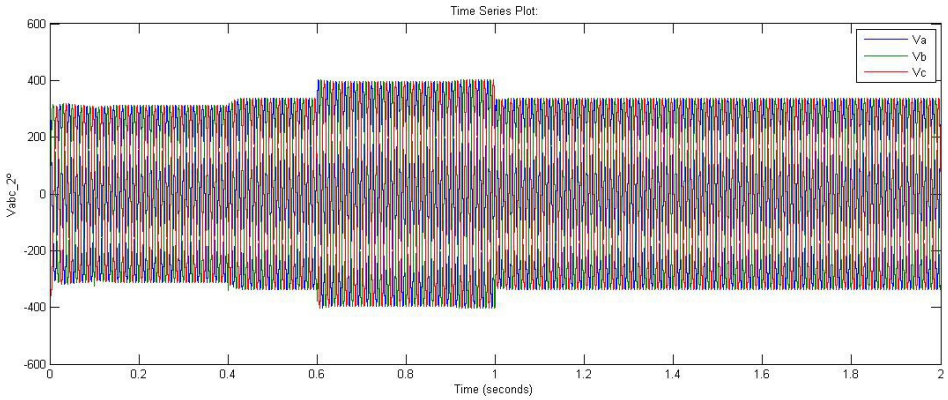

Fig. 33a: Vabc on the transformer secondary side

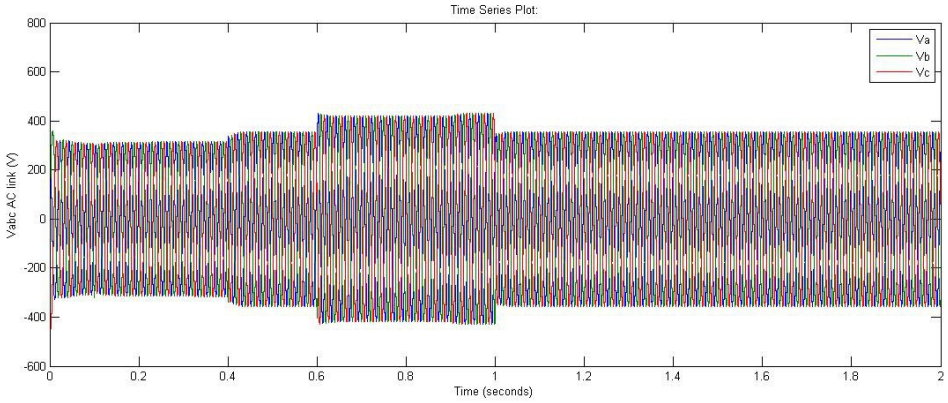

Fig. 33b: Vabc of the converter AC link (before the RL branch)

Looking at the figures 33a and 33b the voltage drop from the AC link of the converter to the secondary side of the transformer is very minimal (almost none).

Afterwards, the transformer steps down the voltage to finally reach the AC grid values.

A second simulation is tried using a value for the transformer secondary side phase to phase rms voltage of Vp_rms = 200 V. Here, the transformer steps up the voltage, since the bigger the relation of the winding voltages (v1/v2), the higher the primary voltage will be in comparison to the secondary (The results are not included for being too repetitive and unnecessary)

Chapter 4: Concluions

Voltage Source Converters are useful in many applications such as distributed generation grids.

For that reason, the structure and operating principle of the two-level three-phase VSC has been studied more thoroughly, and some of its applications like the distributed renewable energy generation, and the storage system and their respective control schemes have been simulated and reviewed.

Finally the three-phase dual active bridge converter (DAB3) has also been mentioned as another application using self-commutated converters and medium frequency transformers in its conversion process to inject power to Medium Voltage DC (MVDC) collection grids. A model with a VSC and a transformer has also been implemented in order to see the effect of the different possible configurations of the transformer to the AC grid's values, and to further understand its operation principle on other applications like the DAB3.

The working principle of each of the VSC's phase has been seen in detail where it is clear that each arm made of two IGBTs and two antiparallel diodes creates one of the three different phases, and how the commutation of the switches injects a positive and negative current alternatively, turning a DC signal into an oscillating one.

Due to its main feature, its self-commutated nature, the VSC can be controlled to have a good harmonic performance and therefore, to be less filtering needy, and thus making them smaller and more compact.

For these reasons, the VSC is good in the following applications:

- Locations where space is at a premium like offshore platforms (compact)
- Applications where power is interchanged with a grid with multpile other connection points.

On the other hand, the disadvantages of this technology in comparison to the classic Line Commutated Converters (LCCs), are that losses will be higher due to the high frequency operation demanded to the IGBTs, and also, Electromagnetic Interferences (EI) due to the series connection of multiple IGBTs on each arm in order to achieve higher voltage values in the case of High Voltage DC (HVDC) applications.

Both simulations have yielded similar results. The current loop regulates the d and q currents, and in the case of the distributed generation system, the dc voltage regulator also

manages to stabilize the DC bus voltage to around 800 V.

Finally, the results of the transformer simulation have been shown and its meaning has been explained.

Chapter 5: Time management planning.

The time management plan used for this project is based on structuring the tasks that must be started or done in the time unit that is each month leading up to the project's turn in date.

February planning:

- Installation of Matlab, and Simulink on the computer.
- Trial of simple simulink models recommended by the tutor in order to get familiarized with simulink and also with the Simpowersystems power electronics library that will be often used in this work.
- Documentation in order to understand and learn the tools and the concepts needed to work on this project [6], such as the components of a wind power generator converter like the Voltage Source Converter, but also concepts like the Park, and Clarke transformations, which are key in order to be able to simplify the said control.

March planning:

- Creation of an initial and simplified model for what will later be the Voltage Source Converter.
- Connection of the Voltage Source Converter model to another model acting as a typical 50 hz electrical grid.
- Implementation of the Voltage Source Converter's control, in order for it to handle a fluctuating generation source.
- Running of the first simulations, and first numeric and graphic results being obtained.
- Initial stages of the document's confection.

April planning:

- Implementation of a more complex control scheme (Q* and Idc* as references).
- Trial and error period in order to eliminate unwanted errors and ripple values. Also to eliminate the algebraic loop created by the control.
- Continuation of the drafting and improvement stage of the written document
- More in depth organization of the written memory's structure and content.

May planning:

- Addition of the transformer to the model.
- Prolonged trial and error period in order for the new model with the added transformer to work and the new formed algebraic loop to be eliminated.
- Continuation of the document drafting process. Special focus on the parts already tackled until that point.

June planning:

- Simulation of the different models and controls.
- Analisis and extraction of conclusions from the results obtained with the different simulated controls.
- Drafting of the conclusions, and finalization of the thesis confection.
- Attainment of the document's physical version and burning of the four CD copies.

Chapter 6: Project budget.

This section is meant to summarize the monetary costs of doing this project, but also its time costs.

Monetary costs:

In order to be able to make this project, it is mandatory to buy one of the latest versions of the Matlab software with Simulink included. Since it is preferable to have the 2013 version or newer, in case of not already having it, its cost is of 70 €.

The printing and binding of the physical copy of the tesis will have a cost of around 20 € depending on each specific place prices.

Finally, the burning of the four CD copies will also be an added price of 10 € on average.

In conclusion, if adding up all those things, the cost goes up to an average of 100 € approximately.

Time investment:

In order to do this project, the approximated time needed is on the order of an entire semester of regular work, including the documentation process, meetings, actual project work and drafting of the memory.

This project is quite time consuming, and the twelve credits of twenty-five hours each, estimated as necessary to complete the project, which in turn add up to a total of three hundred hours, is not too far off the mark in this case.

Bibliography

[1] MATLAB and Simulink for Technical Computing - MathWorks España. (n.d.). Retrieved June 26, 2015, from http://es.mathworks.com/

[2] HELUKABEL GmbH, "Helunews," Newsletter, 11 2011. [Online]. Available: http://www.helukabel.de/media/publication/de/cor_docs/ge_23/GE_COR-DOCS_HELUnews-5_EN.pdf

[3] S. Kenzelmann, "Modular dc/dc converter for dc distribution and collection networks," Ph.D. dissertation, Laboratoire d'Electronique Industrielle, Ecole Polytechnique Federale de Lausanne, 2012.

[4] D. Williams and J. Philips, "Wind in our sails," European Wind Energy Association, Tech. Rep., 2011.

[5] Soltau, N., Stagge, H., De Doncker, R. W., & Apeldoorn, O. (2014). Development and demonstration of a medium-voltage high-power DC-DC converter for DC distribution systems. *2014 IEEE 5th International Symposium on Power Electronics for Distributed Generation Systems (PEDG)*, (978), 1–8. http://doi.org/10.1109/PEDG.2014.6878696

[6] Gomis-bellmunt, O. (2012). Active and Reactive Power Control of Grid Connected Distributed. *Modeling and Control of Sustainable Power Systems: Towards Smarter and Greener Electric Grids*, 47–81.

[7] Monrovia, Y. (1971). Pulse-width modulation. *US Patent 3,630,304*, (October), 2000. Retrieved from http://www.google.com/patents/US3630304

[8] Smart Grid Concept and Characteristics | EEP. (n.d.). Retrieved July 1, 2015, from http://electrical-engineering-portal.com/smart-grid-concept-and-characteristics

[9] C. Meyer, "Key components for future offshore dc grids," Ph.D. Dissertation, Institute for Power Electronics and Electrical Drives, RWTH Aachen University, 2007.

[10] L. Zhang et al., "A modular grid-connected photovoltaic generation system based on

dc bus," IEEE Transactions on Power Electronics, vol. 26, no. 2, pp. 523 –531, feb. 2011.

[11] H. Akagi, Y Kanazawa, and A. Nabae. Generalized theory of the instantaneous reactive power in three-phase circuits. International Power Electronics Conference, pages 1375-1386, 1983.

[12] Three Phase Transformer Connections and Basics. (n.d.). Retrieved July 5, 2015, from http://www.electronics-tutorials.ws/transformer/three-phase-transformer.html

[13] Understanding Vector Group of Transformer (part 2) | EEP. (n.d.). Retrieved July 5, 2015, from http://electrical-engineering-portal.com/understanding-vector-group-transformer-2

[14] 2-level-animation.gif (600×300). (n.d.). Retrieved July 5, 2015, from https://upload.wikimedia.org/wikipedia/commons/2/28/2-level-animation.gif

[15] «Característica idealizada de un transistor bipolar» from Yves-Laurent derivative work: Phirosiberia (talk)